Detailed Modelling of Catalytic Partial Oxidation Processes

Maria Isabel Luiz Gomes Pereira Coutinho[1]

[1] *Instituto Superior Técnico, Universidade de Lisboa, Portugal*

Abstract— Reactor modelling has previously focused on fluid dynamics, using simplified kinetic rate expressions. Although this method has proven to be sufficient in the past, it has a limited range of applicability. This limitation hinders various ends for which reactor models are created: sizing, optimisation, control, etc. This work aims to use detailed microkinetics of the intervening reactions in a catalytic partial oxidation process to generate a comprehensive reactor model. The use of a detailed model for the reaction's kinetics additionally provides a better understanding of the reaction's mechanism and the impact of specific changes on the overall scheme. A microkinetic model for ethylene epoxidation was selected from literature. The detailed kinetics were tested within a gPROMS ProcessBuilder catalytic multitubular fixed bed reactor. A parameter estimation was performed using experimental data. An enhanced model adapted to industrial catalysts was parameterised accordingly. The last stage focused on possible model extensions. The moderator effect and catalyst deactivation were studied due to their prevailing presence in an industrial setting. A deactivation expression was developed for the current microkinetic model, as well as suggestions on incorporating the moderator effect.

Keywords: Ethylene oxide production, ethylene partial oxidation, ethylene epoxidation, microkinetics, modelling, gPROMS

Introduction

Chemical production plants have long been a source of great profit. The search for the most lucrative plant design has progressively become more competitive. Methods for sizing and designing the various equipment, as well as the plant as a whole, have evolved to reach near optimal configurations. Nonetheless, obtaining optimal configurations represents a higher challenge for a few sets of processes. This is the case of the processes that involve catalytic partial oxidation (POX) reactions [1] which leads to most POX processes currently still operating far from optimal conditions, prompting oversized reactors, sub-optimal productivity, and profit loss.

The difficulty in the exact characterization of these processes stems from the fast nature of the POX reactions coupled with the fact that most have accentuated thermal effects. Since the majority of these reactions occur appreciably fast, they often become mass-transfer limited under industrial production conditions, accounting for the unknown kinetics for that range (e.g. CO oxidation) [1].

The POX high exothermic attribute confers numerous complications, including possible safety concerns in respect to run-away reactions and/or regular operating conditions; the need for intensive heat transfer and thermal stability; and the formation of gradients within the catalyst which may achieve steady-state multiplicity [1].

The demand for a detailed model of these partial oxidation reactions arises from the necessity of uncoupling the determination of reaction kinetics from the sizing of the reactor. Simultaneously, it provides comprehensive and exact knowledge of the reactor, allowing to accurately predict the reactor's performance for a wide range of operating conditions, and enabling the optimisation of the reactor's design with scarcely any additional data. As an example of a partial oxidation reaction, ethylene epoxidation was chosen, due to ethylene oxide's prominent growing demand and to the reaction's complex kinetics. Moreover, the microkinetic approach has been successful for similar applications, namely the partial oxidation of methanol to formaldehyde [2].

Ethylene oxide (EO) is the simplest cyclic ether. One of its most hazardous properties, being a very reactive compound, is simultaneously the main reason for its popularity [3]. This aspect enables this chemical intermediate to be applied in a variety of chemical reactions, increasing its demand throughout the chemical industry.

Some of its primary uses include disinfectants, sterilizing agents and fumigants [3]. In respect to the derivative uses, the most significant industry is ethylene glycol production, which is used in applications such as antifreeze and manufacturing polyester fibers. Other derivatives include amines and polyethylene glycols, triethylene glycol, ethylene glycol ethers, ethanolamine and ethylene carbonate [3–5].

Ethylene partial oxidation competes with other two reactions, ethylene and ethylene oxide total oxidation, as shown in Fig. 1. Thermodynamically, total combustion is markedly more favourable; ethylene oxide is only the kinetic product [6].

Previous modelling approaches focused on obtaining the extent of each one of these three reactions through rate expressions. The expressions could be power-laws [4] or Langmuir-Hinshelwood-Hougen-Watson (LHHW) formula-

Contact data: no. 81788, Chemical Engineering Master's Degree
isabel.p.coutinho@tecnico.ulisboa.pt

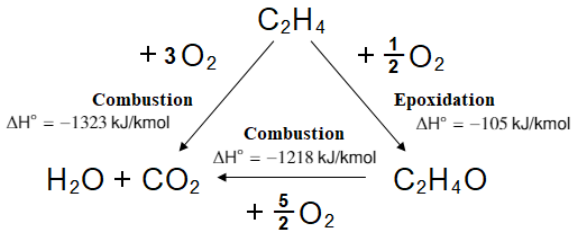

Fig. 1: Simplified ethylene oxidation scheme

tions [7–13], both with fitted parameters. However, the proposed detailed modelling involves using a reaction mechanism. The discrimination of the intermediate steps for each reactions provides a deeper understanding of the reactions and their respective driving forces. Additionally, it establishes the nature of the relationships between the three main reactions.

Although thoroughly investigated, the scientific community has not reached a consensus for the mechanism that entails ethylene partial oxidation [6, 10, 14]. Early mechanisms established molecular oxygen as the only active oxygen species [3, 15]. This implied that there was a 6/7 upper bound for epoxidation selectivity. It was stipulated that combustion displayed an ensemble effect, which dictated that this reaction required a larger amount of sites to occur [16]. At the time, all experimental data corroborated this mechanism. More recently, promoted catalysts have reached selectivies as high as 90 %, disproving this theory [3, 16].

Authors Grant and Lambert [17] proposed the presence of two types of adsorbed oxygen: a low-valence charge "selective" oxygen and a high-valence charge oxygen (which took part in hydrogen abstraction) [18].

Reports of the existence of three types of oxygen [5, 6, 16, 17, 19]: adsorbed atomic oxygen, subsurface atomic oxygen and molecular oxygen, are fairly universal. The subsurface oxygen is usually described as adsorbed oxygen that has migrated into lattice positions.

Recent developments in this field has evolved to believe that the subsurface oxygen is an active species in the process [3, 5, 17]. Its contribution is thought to be the removal of electron density from the silver particles which are bonded to the atomic oxygen, providing an electrophilic character to the metal-adsorbate compound. This promotes the interaction of the adsorbed oxygen with the ethylene C-C bond by drawing electron density to the catalyst's surface [3, 5, 20, 21].

Waugh an Hague's [22] investigation on kinetic parameters provided additional insight on the mechanism. By observing that both epoxidation and combustion have similar activation energies, it is considered that a possible common intermediate to both reactions may be present in one of the rate-determining steps [6, 16, 22–24]. They also enlighten on the role of the cesium promoter, which inhibits the formation of the unselective silver-oxygen bonds.

Linic and Barteau [25] combined Density Functional Theory (DFT) calculations and High-Resolution Electron Energy Loss Spectroscopy (HREELS) experiments to prove the existence of an oxametallacycle intermediate, using the reversibility of the reaction. Its vibrational presence in the infrared spectrophotometer had been previously recorded by Force and Bell [26]. This has been considered to be the common intermediate previously postulated.

The predominate belief is that the oxametallacycle intermediate forms either ethylene oxide or acetaldehyde. The latter is then readily combusted, generating the unselective pathway [6, 27, 28].

Generally, the rate-determining step under industrial conditions has been set as the dissociative chemisorption of oxygen [5, 25], although the same may not be applicable in other temperature and pressure ranges. In contrast, Grant and Lambert [17] reported the surface reaction as the rate-limiting step.

The catalyst usually elected by the industry is silver finely dispersed (7-20 %) on a porous matrix (pore diameter within 0.5 to 50 μm) of α-alumina (higher than 99 % purity) [3, 6, 16, 25]. It has low specific surface area (around 2 m^2/g) [3, 5, 6] which confers less activity but higher selectivity, and slows down diffusion to inhibit further oxidation. Hydroxyl groups must be removed from the support through silane treatment to avoid promoting catalytic isomerisation to acetaldehyde. The catalyst is used in the form of spheres or rings with diameters that range from 3 to 8 mm [3].

Promoting the catalyst with alkali salts has become widespread [3, 5, 29], usually in the range of 100-500 mg/kg. It is noteworthy that residual acidity in the support is highly unfavourable for the process selectivity, since it promotes the combustion reaction [5]; hence the need for the previously mentioned alkali salts, (which reduce density of acid sites). These also enhance oxygen dissociation [5].

Cesium or a combination of rhenium, sulfur, tungsten and molybdenum can significantly affect the selectivity, which may thus reach the 80 % threshold. Cesium is said to create a silver film that decreases the support's importance [23, 30, 31], and increases the selectivity.

The use of chlorine-based modifiers [3, 5, 16, 29, 32–35] is also of the utmost importance. These compounds (e.g. 1,2-dichloroethane (DCE), vinyl chloride (VCM), and ethyl chloride) are added to the reactor's feed to provide a higher selectivity for the epoxidation reaction, while simultaneously decreasing the rate of both epoxidation and combustion reactions [5, 16, 34].

The method of how these moderators work is still uncertain, although their positive effects are clear throughout literature [34]. There are two major (non-exclusive) theories of how these modifiers promote the selectivity. The first consists of enhancing the electrophilic effect of silver [5, 25, 32]. It can be considered as the modifier, acting as a surrogate for subsurface oxygen, since chlorine atoms draw electron density from the metal surface, or as the rehybridization of valence band orbitals [32]. This is supported by the increase in apparent heat of adsorption reported by ethylene at higher modifier concentrations [16].

The second theory considers that chlorine acts as a suppressor [5, 32], occupying vacant sites that neighbor the intermediates and preventing total oxidation to occur. The latter site-blocking theory is corroborated by the fact that at high concentrations chlorine becomes an inhibitor, poisoning the catalyst and preventing oxygen chemisorption [24, 32].

Other authors [3] state the modifiers ensure an even coverage.

In regard to the reactor, high reaction heats account for the

need for efficient means of heat transfer, at times considered the determining process in the reaction kinetics [4, 6]. Multitubular arrangements with coolant circulation through the shell-side are therefore employed for this purpose. The inlet is fed in gas-phase, with the alternative of air and oxygen-based processes [3, 5]. Reaction temperatures and pressures range from 230 to 290°C and 1 to 3 MPa, respectively [3, 5, 6].

The tube bundles consists of thousand of tubes which are 6-13 meters long and have 20-40 mm internal diameter (to ensure proper heat transfer). The catalyst is located inside the tubes [3].

Mild steels (e.g. stainless steel) are used in the reactor even though ethylene oxide is not corrosive since the process may reach relatively high temperatures. Additionally, this prevents rust, which promotes isomerisation, polymer formation, and increases the viscosity [3, 16].

Modern designs use pure oxygen in a single-stage apparatus [5]. Recycling of recovered reactants is standard to ensure acceptable process yields and to increase profit. The reactors' feed has a high ethylene content (25-30 %), and the oxygen content is subject to the reaction mixture remaining above the upper flammability limit [5, 6, 16]. This new configuration achieves overall higher yields in smaller equipment [5].

Various processes may lead to the deactivation of the Ag-based catalysts, the most significant being sintering, poisoning (e.g. sulfur from ethylene) and wearing [33, 36]. Processes such as abrasion and dust formation are adverse for the stability of the catalyst [3].

The commonly employed solution to counter-effect the loss of activity due to sintering is to increase the reaction temperature [34, 36]. In practice, plants gradually increase feed or coolant temperature to compensate for this aging effect of the catalyst, since the silver surface decreases to 50 % its initial value in two years [3]. However, there is an upper limit for the feed temperature (flammability limits): when this condition is reached, the catalyst must be replaced. The frequency of catalyst replacement is dependent on the type of catalyst, the rate at which the process is run, and the purity of the feed. In general, highly selective catalysts require to be traded every 2 years, while lower selectivity catalysts last for 5 years [3].

Surface Reaction Microkinetics

Stegelmann et al. [6] have created a microkinetic model for unpromoted silver with parameters obtained from transient surface science experiments in UHV and steady-state kinetics on single crystals. It reports the presence of two types of active sites: silver metallic silver sites (*) and surface oxide sites (O*). It further describes the adsorption of oxygen from an oxide layer, which results in surface reconstruction: these events are corroborated by DFT and ab initio calculations and laboratory experiments [6]. This model is consistent with oxygen adsorbing more strongly on pre-oxidized surfaces [6, 14, 37–40]. Furthermore, the model corroborates the predominate theory of an oxametallacycle intermediate for both selective and unselective reactions.

Species may be adsorbed in * and O* sites, generating what Stegelmann et al. [6] coined as *surface species*. These adsorbed species, in addition to the gaseous components, are the reactants/products of the reaction steps (see Table 1 Ref. [6]).

The main limitation reported for this model is the underprediction of activity below the oxygen partial pressure of 10 kPa [6]. Product inhibition was al so neglected since only initial rates were considered [6].

Partopour and Dixon [27] have successfully simulated the microkinetics proposed by Stegelmann et al. [6] using CatalyticFoam.

The reaction scheme presented by Stegelmann et al. [6, 37] was used in this work. Stegelmann et al. [6, 37] developed a 17-step scheme (see Table 1 Ref. [6]) for ethylene epoxidation, which incorporates the two secondary (undesirable) reactions: ethylene and ethylene oxide combustion.

Although the gPROMS ProcessBuilder reactors are coded to allow for user-defined kinetics, the template is designed for power-law or LHHW-type rate expressions. For this reason, a microkinetics custom model was created in order to enable the simulation of a multi-step reaction.

The rate of each step i at temperature T is given by eq. (1).

$$r_i^T = k_i^{forw,\,T} \prod_l^{RR} \left(\frac{p_l^a}{P_{ref}} \cdot \theta_l^a \right) - k_i^{rev,\,T} \prod_l^{P} \left(\frac{p_l^b}{P_{ref}} \cdot \theta_l^b \right) \quad (1)$$

$$k_i^{j,\,T} = k_{0,\,i}^j \cdot e^{-\frac{E_i^j}{RT}} \quad (2)$$

Where r_i^T is the overall reaction rate for step i at temperature T, $k_{0,\,i}^j$ is the pre-exponential factor in the direction j (forward, reverse), $k_i^{j,\,T}$ is the rate constant, E_i^j is the activation energy, p_l is the partial pressure of component l, P_{ref} is the reference pressure, θ_k is the surface coverage of species k, RR and P represent reactants and products, respectively, and a and b represent the stoichiometric coefficient at which RR and P react/are produced, respectively.

The surface coverage, θ_k, of the surface species k is the fraction of active sites (*) that have been occupied by the given species. As a result, the sum of coverages must be equal to 1. To determine the coverages, the following mass balance was written:

$$\frac{\partial \theta_k}{\partial t} = \sum_k \left(\beta_1 \cdot r_{k\ is\ produced} - \beta_2 \cdot r_{k\ is\ consumed} \right) \quad (3)$$

where β_1 and β_2 are the stoichiometric coefficients of surface species k in the step it was produced and consumed, respectively.

There is an Arrhenius temperature dependence for the reaction constants (eq. (2)). Therefore, the rates, and necessarily the surface coverages, are temperature dependent. Furthermore, the rates are a function of the partial pressures at a given point.

The pre-exponential factors (k_0) and activation energies (E) were obtained from literature (see Table 8 Ref. [6]).

The use of elementary steps eliminates the concept of overall reactions between the gas species. Since mass balances in the catalyst pellet models consider only the gas phase components, reactions for production/consumption of all the gas components were defined independently as the sum of the reaction steps in which they intervene.

$$RRate_{rr} = \phi \cdot \rho_* \cdot \sum_{i}^{\text{Step 17}} (\beta_{i,m} \cdot r_i) \tag{4}$$

$RRate_{rr}$ represents the rate of reaction rr, ϕ is the effectiveness factor, ρ_* is the density of active sites (mol/kg), r_i is the rate of step i and $\beta_{i,m}$ is the stoichiometric coefficient of component m in this reaction. Each reaction rate is associated with only one component, m.

The reaction scheme proposed by Stegelmann et al. [6] aims to detail all the steps that the reactants undertake to become the products observed in EO production. However, it must be noted that not all the steps considered within the scheme are elementary. This is the case for steps 10 and 14. Due to absence of additional insight on the workings of the mechanism, the authors [6] considered these simplified steps, which are, therefore, void of scientific veracity.

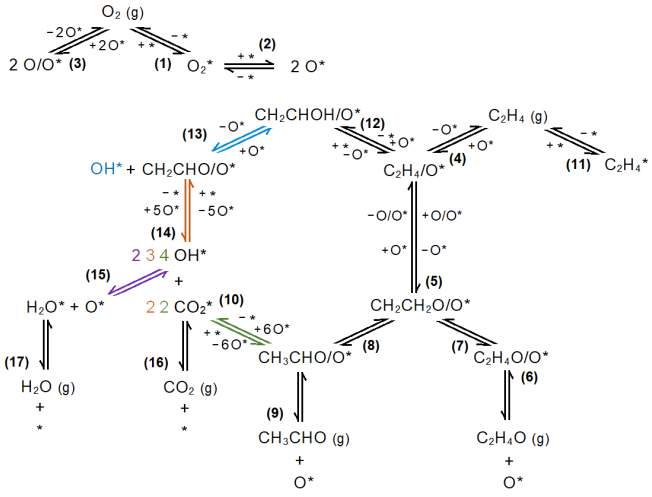

Fig. 2: Schematic representation of the multi-step mechanism[1]

Fig. 2's representation underlines how ethylene oxide production and ethylene oxide combustion may have the same oxametallacycle intermediate ($CH_2CH_2O/O*$). As mentioned previously, this common intermediate has been supported by many articles [17, 41–44]. The isomerisation of the product to acetaldehyde through the oxametallacycle is also included. The ratio between the equilibrium constants for steps 7 and 8 is, therefore, decisive in determining the relevancy of EO combustion.

In addition to ethylene oxide combustion there is a second route to CO_2 and water production (steps 12-14). These steps represent ethylene combustion, which is less meaningful for the current mechanism. Interestingly, authors Partapour and Dixon [27] found these steps insignificant to the extent that they eliminated them completely to create a simplified model.

The steps for the formation of O* (from oxygen) are presented separately, since they impact too many other steps, and would render the analysis of the scheme to be extremely complicated.

[1]The colours mark the stoichiometry and species that intervene in a step. The numbering is done through brackets and placed next to the forward direction of the corresponding step.

The majority of the model parameters were determined, by the authors [6], through surface science experiments and auxiliary calculations, conferring them physical meaning. However, these experiments were performed on single unpromoted crystals, rending its extrapolation to industrial catalyst dubious. Furthermore, the validation that Stegelmann et al. [6] performed used initial rates which do not account for the product inhibition effect to the extent which it occurs industrially.

Thus, the scope of this work is to provide an enhanced model, adapted to industrial catalysts and conditions.

Parameter Estimation

Petkim Petrokimya Holding A.Ş. has provided a series of experimental laboratory trials, in which different reaction conditions were tested. Since the catalysts used in these experiments had different activities from the catalysts used to determine the parameters proposed by Stegelmann et al. [6] it was necessary to adapt the model to the current activity and selectivity.

As was observed previously, model parameters, such as steps 7 and 8 pre-exponential factors, were selected to fit the selectivity on Ag(111). Furthermore, the density of active sites is also particular to the catalyst as it is a measure of its activity. These parameters must be estimated prior to model validation for a coherent comparison.

Each catalyst loading also has a different start-of-run activity which must included in the model. The usefulness of this parameter arises from the non-uniformity of the catalyst batches created. The activity varies (but not substantially) between batches. By establishing a reference batch, the quality of the activation of the remaining can be analysed by comparison. Reference activities higher than 1 translate into a better activation. The latter concept will henceforth be referred to as catalyst reference activity ($\alpha_{ref}^{\rho_*}$), and will be employed in the model generating the site density variable:

$$\rho_* = \rho_{*,0} \cdot \alpha_{ref}^{\rho_*} \tag{5}$$

The data used in the parameter estimation was obtained in a laboratory reactor. Various experiments were carried out with different feeds, and operating temperatures and pressures. These experimental laboratory trials have previously been used and described in a greater extent in Sarrafi's thesis [45].

The reactor itself was scaled-down from industry. In contrast with a plant reactor, there was no fluid used to cool the reactor. It was substituted by a furnace which would heat the miniature reactor to the desired reacting temperature. The set-point of the furnace may have not been achieved in the duration of the experiment. Furthermore, the reactions that took place within the reactor generated temperature profiles along the bed, rendering the set-point to be merely a reference value. The kinetic model used just the center measurement of the catalyst bed, referred to as *Bed Temperature at 10 mm*.

The experiments were divided into different catalyst loading. Catalyst loadings could differ in the amount of mass of catalyst used in the reactor. Table 1 shows the different conditions at which the experiments were performed. The ex-

Table 1: Description of the experiments considered in the parameter estimation [45]

Experiment	Mass of Catalyst (g)	Relative Pressure (kg cm^{-2})	Furnace Setpoint Temperature (°C)	Feed Composition (%mol) (*)					
				C_2H_4	O_2	CO_2	EO	VCM	CH_4
1_1	0.1	0	219	22.74	5.77	4.14	0	0	63.08
1_2		0	237	22.74	5.77	4.14	0	0	63.08
1_3		0	255	22.74	5.77	4.14	0	0	63.08
2_1	0.1	0	219	66.6	1.81	2.1	0	0	29.49
2_3		0	219	25.68	1.81	6.18	0	0	66.33
2_4		0	219	8.53	23.04	2.1	0	0	66.33
2_5		0	219	35.18	14.28	4.28	0	0	46.26
3_1	0.1	0	255	29.76	1.81	2.10	0	0	66.33
3_2		0	255	26.95	23.04	6.18	0	0	43.83
4_1	0.2	0	237	22.74	5.77	4.14	0	0	63.08
4_2		0	219	22.74	5.77	4.14	0	0	63.08
4_3		0	250	22.74	5.77	4.14	0	0	63.08
6_3	0.2	0	237	22.75	5.77	0	0	0	57.34
6_5		0	237	22.75	5.77	4.14	0	0	57.34

(*) Balance with Helium

periments were identified using the following nomenclature: *catalyst loading_experiment number*.

The experiments' feed composition was defined for each trial and are shown in Table 1. These have been calculated by defining the standard volumetric flow of the various feeds. The remaining component in the feed is helium, an inert used to carry small quantities of the EO and VCM.

The experiments measured the temperature along the bed and the outlet dry composition. The latter was obtained by gas chromatography and focused on the five following components: methane, ethylene, oxygen, ethylene oxide and carbon dioxide.

The Orsat composition has subsequently been submitted to a data reconciliation process, where the outlet of methane has been adjusted to ensure carbon balance. The methane outlet composition measurement was then disregarded for the present parameter estimations.

A gPROMS ProcessBuilder flowsheet was created to resemble the experiment conditions and set-up. It included various models, namely, the Stegelmann et al.'s [6] microkinetics custom model.

The controls defined in the gPROMS platform where the variables from the originally defined *Process*, which may change for each experiment. The time invariant controls were the following: the catalyst loading, the mass of catalyst, the relative pressure, and the EO/He and VCM/He inlet standard volumetric flow. The piecewise constant controls were the following: bed temperature at 10 mm and the remaining components' inlet standard volumetric flow.

Additionally, the outlet dry composition of EO and carbon dioxide were the measurements used. Ethylene and oxygen outlet dry composition were observed for monitoring purposes.

To facilitate the parameter estimation, a variable change was performed. The pre-exponential terms were substituted by constants at a reference temperature which was set as 525 K (the furnace set-point for multiple trials). The new parameters were determined using the original ones and the following expression:

$$k_i^{j,T_{ref}} = k_{0,i}^{j} \cdot e^{-\frac{E_i^j}{RT_{ref}}} \tag{6}$$

in which $k_i^{j,T_{ref}}$ is step i's constant at reference temperature in the direction j (forward, backward) and E_i^j is the activation energy for step i in the direction j.

Following various preliminary estimations, the following strategy was applied: the steps identified as rate-determining were estimated (only the forward parameters). This approach had the disadvantage of the substantial amount of parameters it entailed. However it eliminated estimation of parameters that would not have a significant impact on the overall scheme. Due to the amount and nature of the parameters, the existence of correlations and, consequentially, the low confidence of the estimated parameters was expected.

Table 2 confirms the suspected drawback of this approach: there is low confidence in the values estimated. The advantage of this method sets upon its grasp on the selectivity. Contrasting with the previous preliminary estimations, the dry outlet composition predictions of ethylene oxide and carbon dioxide (Fig. 3) are almost a perfect match.

The quality is most visible on the carbon dioxide composition which is predicted with near perfect accuracy. In respect to the EO predictions, it must be underlined that the axis of the graph shows a much more confined range, for which the deviations shown are lower than the 0.1 % magnitude (irrelevant).

Furthermore, the CO_2 produced by ethylene combustion as a percentage of the total produced CO_2 was defined. This

Table 2: Estimated paramters

Model Parameter	Estimated Value	Standard Deviation
$\alpha^{\rho*}_{ref,2}$	1.51	± 0.05
$\alpha^{\rho*}_{ref,3}$	0.98	± 0.03
$\alpha^{\rho*}_{ref,4}$	0.549	± 0.005
$\alpha^{\rho*}_{ref,6}$	1.16	± 0.08
$k_2^{forw,T_{ref}}$ (s^{-1})	6 x 10^7	± 10 x 10^7
$k_5^{forw,T_{ref}}$ (s^{-1})	1153	± 2
$k_7^{forw,T_{ref}}$ (s^{-1})	0.7	± 2
$k_8^{forw,T_{ref}}$ (s^{-1})	0.2	± 2
$k_{13}^{forw,T_{ref}}$ (s^{-1})	19	± 2 x 10^4
E_2^{forw} (kJ/mol)	390	± 2000
E_5^{forw} (kJ/mol)	383	± 50
E_7^{forw} (kJ/mol)	14	± 8
E_8^{forw} (kJ/mol)	98	± 10
E_{13}^{forw} (kJ/mol)	70	± 900

performance indicator was used to investigate the case study consisting of experiments 1_1 and 2_5.

The two experiments (1_1 and 2_5) display the same measured temperature (~504 K). Two identical temperatures will predict the same carbon dioxide production if two routes for combustion are not proposed, having only the temperature dependence of the model as an influence on the selectivity. Intuitively, this is incorrect. It was found that for experiment 1_1, the CO_2 produced through ethylene total oxidation varied from 55 % to 60 % (along the bed). For experiment 2_5, ethylene total oxidation only accounted for 45 to 48 % of the CO_2 produced.

The use of the model provides an explanation for the different measurements reported for these two experiments. It points to experiment 1_1's feed composition being a region in which ethylene combustion is predominant. The same is not applicable to experiment 2_5. Moreover, since the percentage of CO_2 produced from ethylene oxide is established, it is possible to quantify the increase in the selectivity that would be observed if ethylene oxide combustion were to be totally inhibited.

Model Extensions

A gPROMS ProcessBuilder flowsheet was set-up to test possible model extensions using a simplified assembly. The assembly consisted of a catalytic multitubular fixed bed industrial reactor, an inert bed, two coolants, and a stream splitter to dry the effluent.

The first model extension deliberated was the moderator effect. The *Introduction* briefly explained the role of moderators in EO production. It may be stated that rare are the cases which do not use this strategy to increase overall yield

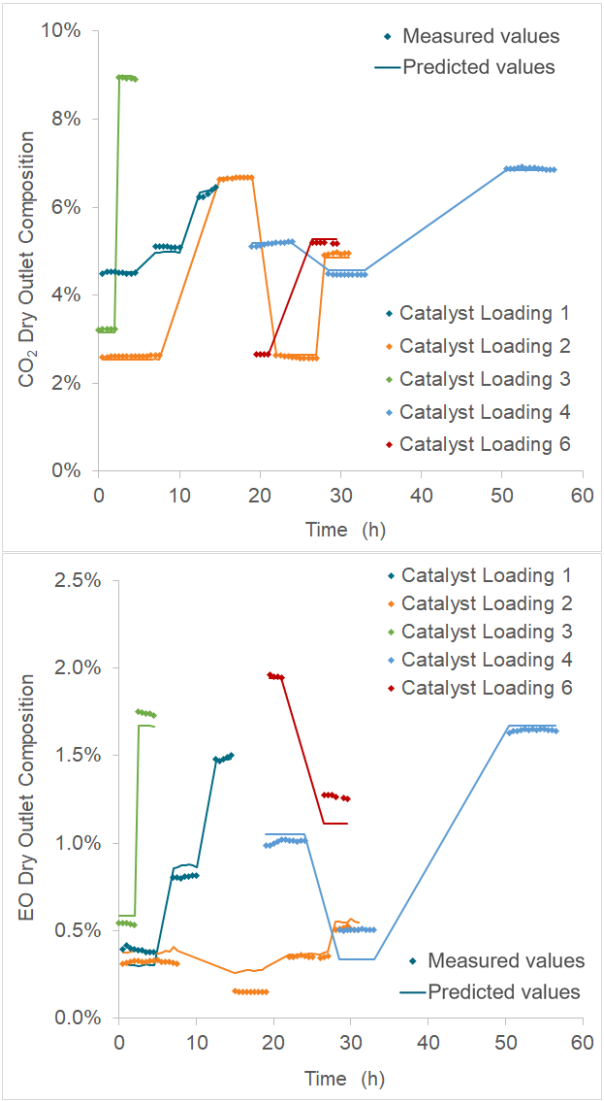

Fig. 3: Catalyst loading 1, 2, 3, 4 and 6's measured and predicted carbon dioxide and ethylene oxide dry outlet composition

from the raw materials and render the process more profitable. Being a crucial aspect in reactor's performance and optimisation, this factor must be included in the scheme.

These compounds are not considered promoters, since they do, in fact, inhibit the reaction (lower the conversion) [46, 47]. Yet, they are added consistently to reactor's inlets, due to their ability to increase the selectivity to the 90 % threshold[2] [48]. These chlorine compounds (VCM, DCE, etc.) are added in vestigial amounts to the streams (few ppm), and still have a substantial impact [35, 48]. As a case study, vinyl chloride (VCM) was studied.

The goal of this section was to insert in Stegelmann et. al.'s [6] model the moderator effect as a physical phenomenon (non-empirical form) to maintain consistency with the overall tone of the scheme. However, as was underlined in the *Introduction* section, there is no universal agreement in the scientific community of how the modifiers operate.

The first option examined was chemisorption. Since the presence of VCM is said to both increase the selectivity and decrease the conversion, the purpose was to find an adsor-

[2]Valid for promoted catalysts which show a 80 % selectivity before this addition [23, 30].

ption that met these two goals. The most potential was accommodated by the oxide sites (O*). The incorporation of a step 18 (eq. (7)) would represent the adsorption of the moderator on the vacant oxide sites. Adsorption on the oxide sites causes the coverage of O* to decrease by generating a new surface species, VCM/O*.

$$\text{VCM (g)} + \text{O*} \rightleftharpoons \text{VCM/O*} \tag{7}$$

By analysing the reaction scheme (Fig. 2), it may be observed that the decrease in O* coverage decreases step 4, which is the reaction that defines the consumption of ethylene (since step 11 is ate equilibrium), thus achieving the first goal.

Another observation is that steps 10 and 14 are highly dependent on O* coverage, consuming 6 and 5 O*, respectively. These two reactions are the steps which produce the adsorbed combustion products (CO_2* and H_2O*). Therefore, decreasing these steps increases the selectivity by inhibiting the combustion reactions.

Furthermore, steps 12 and 13 are also inhibited (in a lower extent) by the decrease of oxide coverage. These steps (along with step 14), form the path for ethylene combustion, which is an unwanted side reaction, increasing, once more, the selectivity.

Finally, the low coverage of oxides would promote the desorption of ethylene oxide (since it produces a vacant O*), also increasing the selectivity.

Different adsorption constants and activation energies for step 18 were tested. Although the proposed adsorption gathered all the necessary conditions, the results were not satisfactory. The simulations showed that lowering the O* coverage had a much more severe impact on ethylene conversion than on EO selectivity. It was observed that the conversion reached values below 1 % before any real change in the selectivity could be registered. Even so, the values of selectivity were still far below what was expected. Furthermore, industrial values report selectivity increasing to 90 % (for promoted catalysts), while the conversion remains in the 7-15 % window [48]. When analysing the results, several factors were outlined.

Step 4 is determined solely by the availability of oxide sites, since there is an excess of ethylene present. This is closely related to oxygen being the limiting reactant and explains the denoting change in the conversion.

Secondly, steps 10 and 14 are not actually dependent on the availability of oxide sites (since they are irreverible), hence the sharp decrease in these steps being unachievable. Their irreversible nature stems from markedly high forward constants (in the 10^{20} s^{-1} order of magnitude) which have been set (by Stegelmann et al. [6]).

Although unsuccessful, the simulation of VCM adsorbing on oxide sites breeds interesting questions. Namely, is the path drawn by the authors for ethylene combustion the best approach? Surely, it is fairly adequate to describe the surface reactions, as was observed in the *Parameter Estimation*. Nevertheless, one must also consider the alternative that the original reaction scheme proposed by Stegelmann et al. [6] is, in fact, correct. In this note, the best approach is to move on to the Ag-bonding phenomenon.

In this approach, VCM works as a surrogate for subsurface oxygen, providing the silver-oxygen (atomic) intermediate the electrophilic character that promotes epoxidation. This theory has been proposed by literature [5, 16, 25, 32].

The alternative step 18 is presented by eq. (8).

$$\text{VCM (g)} + \text{*} \rightleftharpoons \text{VCM*} \tag{8}$$

Incorporating the electrophilic effect provided by the VCM is more trying. In theory, VCM-Ag bonding would promote some steps and inhibit others. The proposed effect is simple in theory, but too complex to apply at this stage.

The premise is that all the steps which involve * in the original scheme develop a twin step, identical to the originals, but using VCM*. These steps would have different temperature dependence and rate constants.

The challenge is presented by this astronomical amount of new parameters suggested by this proposal: 18 new steps (17 twins and the step presented by eq. (8)) with 4 sets of parameters each (forward and reverse activation energies and pre-exponential constants). To apply this proposal at this stage would result in a highly-empirical model, since the number of added parameters is hefty, with no known constraints. It remains as a suggestion that will be further detailed in the *Future Work* section.

The second model extension studied was the catalyst deactivation. The model had to be adapted to support the loss of activity with time. This concept is known as catalyst deactivation. The deactivation of a catalyst may have various causes. Poisoning or deposition on the surface of the catalyst, changes in oxidation state of the catalyst's metals and sintering, are common examples [49]. Although all the previous types of decay may impact the present catalyst, the latter is the most predominant effect [50, 51]. For this reason, a sintering instigated deactivation was added to the model.

Sintering is a temperature activated phenomenon, which promotes the formation of particle clusters, decreasing metal dispersion in the catalyst. The Ag/α-alumina catalyst is exposed continuously to very high temperatures for a prolonged period of time in the ethylene oxide production process, hence the sintering effect being prominent.

An advantage of using a detailed model is, once again, highlighted by this situation. In other models deactivation would be included directly into the rate expression(s). Although this would be computationally less demanding, the oversimplification rids the expression of what could be an opportunity to allocate scientific meaning to parameters.

In the present case, the loss of dispersion (caused by sintering) may be allocated to the parameter site density. Since this model parameter represents the number of free active sites available to adsorb (*), these will naturally decrease in number (of availability) if the clusters prevent molecules from contacting with all the metal particles.

A standard general power-law expression, eq. (9), proposed by Bartholomew [52], was used:

$$\frac{\partial \alpha}{\partial t} = k_d(\alpha - \alpha_{terminal})^m \tag{9}$$

$$k_d = k_{d,0} e^{-\frac{E_d}{R}\cdot(\frac{1}{T}-\frac{1}{T_{ref}})} \tag{10}$$

in which α represents the catalyst activity, $\alpha_{terminal}$ is the terminal activity, k_d is the deactivation kinetic constant (which

follows a standard Arrhenius temperature dependence, eq. (10)), and m is the deactivation rate order.

This expression accounts for the deactivation being a temperature promoted occurrence. Higher temperatures result in higher deactivation rates which is compatible with sintering. Furthermore, it has another important factor: terminal activity. Contrary to reality, many deactivation expressions consider that the activity of the catalyst can reach 0. This expression, however, considers an end-of-life activity. An activity to which the decaying catalyst tends, observed for industrial catalysts [36, 50].

Applying the previous expression to the site density, a new variable is generated:

$$\rho_* = \rho_{*,0} \cdot \alpha^{\rho_*} \tag{11}$$

Interestingly, a wide number of implications are drawn from the previous expression. For once, the site density becomes a distributed variable, since α^{ρ_*} is temperature-dependent, and temperature varies along the bed. Secondly, at time 0 the activity of the catalyst is defined using the scalar $\rho_{*,0}$ and the $\alpha^{\rho_*}_{t=0}$. The latter has been formerly introduced as the catalyst reference activity ($\alpha^{\rho_*}_{ref}$).

The value of m was fixed as 2 for this is the most common deactivation rate order and simultaneously the one used in Zhou and Yuan's article [33]. The site density deactivation constant pre-exponential factor ($k^{\rho_*}_{d,0}$) was fixed with one of the values proposed by Zhou and Yuan (see Table 4 Ref. [33]) and possible values for $E^{\rho_*}_d$ were examined.

Increasing coolant temperature is a commonly employed strategy in plants to maintain the conversion as the catalyst deactivates progressively. The method to determine a feasible $E^{\rho_*}_d$ consisted on finding the value which would result in a coolant temperature increase of 35°C (approximately) in 4 years, at constant conversion. Thus, a simulation was run which replaced the conversion degree of freedom with the inlet temperature of the coolant. The value obtained was 155 kJ/mol.

An analysis of the effects of this deactivation energy to the key performance indicators (KPIs) was also performed. This analysis used constant coolant temperature (Fig. 4).

There is a visible decrease in the conversion, as intended. Its trend is within expected, for it reaches the 5 % deactivation barrier. Most importantly, there is only a residual change in the selectivity (increases slightly, approximately 0.15 pp). Reports on the deactivation having a discernible effect on the selectivity have been seen throughout literature [36, 49, 50]. Thus, the need for a second handle (that will tune the selectivity) to be in place arises. At this stage it is unknown if this second handle is truly required, or if this residual effect is considered sufficient. Nonetheless, it is important to create the option.

The expression used in eq. (9) was used once more, in this instance to deactivate the combustion reaction via step 8. The ratio between the reaction rate for steps 7 and 8 is crucial in defining the selectivity.

$$r_8 = r_{8,0} \cdot \alpha^{comb} \tag{12}$$

Three deactivation energies (using similar values to the ones obtained for site density deactivation) were tested for the present deactivation. The pre-exponential for the combustion deactivation was set to the same value as the site density's.

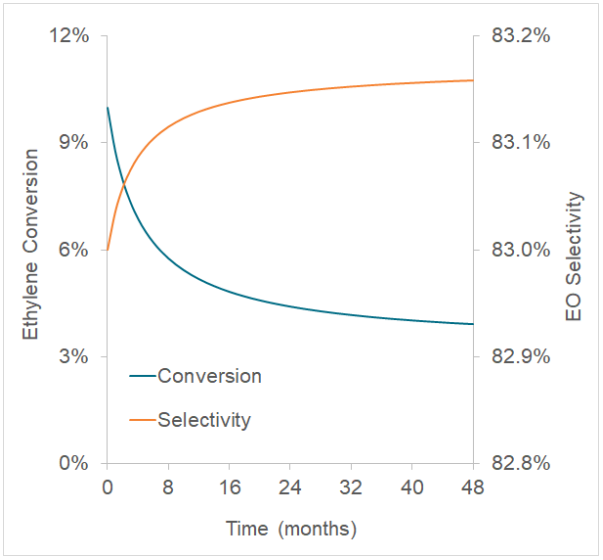

Fig. 4: Change in the conversion and selectivity due to site density deactivation using $k^{\rho_*}_{d,0}$ = 4 x 10^{11} months^{-1} and $E^{\rho_*}_d$ = 155 kJ/mol

The simulation results (Fig. 5) show positive outcomes which may be observed firstly on the conversion. The conversion graph shows a nearly identical behaviour for the various deactivation activation energies tested. Thus, it may be reported that the handle selected for the selectivity deactivation will not have a significant influence on the conversion; which facilitates the tuning of these parameters since there is little internal interference.

The second observation uses the selectivity graph as visual aid. It is possible to identify that the activation energies shown have all marked impacts on the present KPI. Yet, they all follow utterly distinct trends to which the catalyst reaches its terminal selectivity.

Both these observations lead to the conclusion that if a handle on the selectivity is considered advantageous, the proposed strategy is successful in adapting to a plethora of deactivation trends. Furthermore, these two handles may be easily employed, demanding merely experimental data.

Conclusions

Modelling is a potent and extremely versatile tool. It enables the sizing of equipment, the optimisation of conditions, and the creation of control strategies. Particular attention must be given to modelling the reactor, since this is often the core of a process. Most reactor modelling approaches have focused on fluid dynamics. Indeed this has been the major tactic for ethylene epoxidation [4, 27].

This work uses microkinetics to describe the reactions that take place within the reactor. Rate expressions based on Langmuir-Hinshelwood formulations, power-laws or equivalents are the usual treatment for the reaction kinetics. This approach is sufficient for many reactions. However, due to its complexity, catalytic partial oxidation reaction modelling is significantly improved by the use of microkinetics.

A mechanism for ethylene epoxidation was selected from

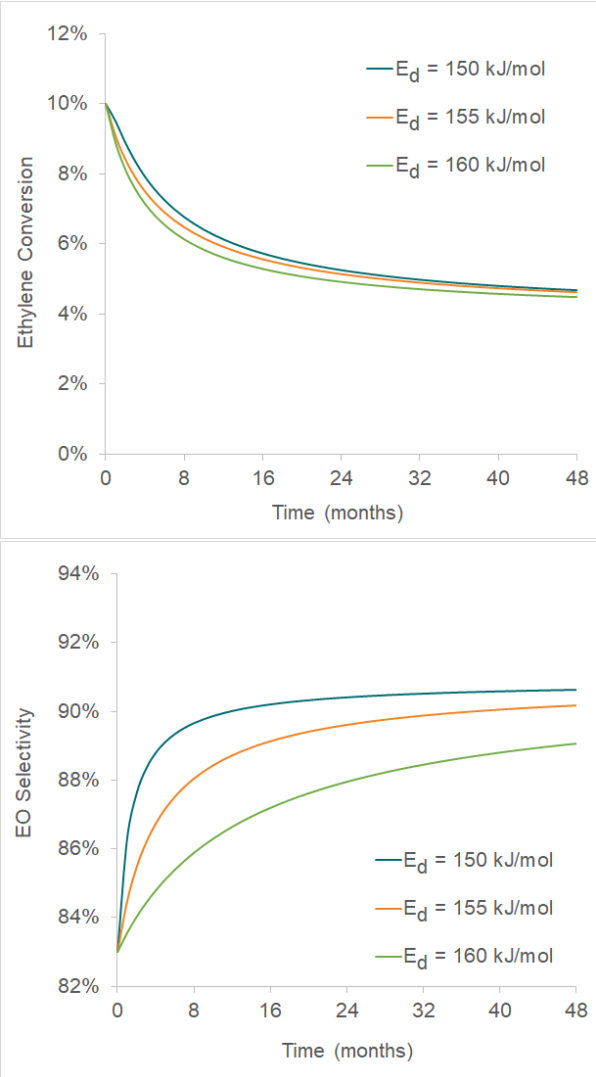

Fig. 5: Change in the conversion and selectivity due to combustion deactivation using $k_{d,0}^{comb}$ = 4 x 10^{11} months^{-1} and E_d^{comb} = 150, 155 and 160 kJ/mol

literature. The reaction scheme was proposed by Stegelmann et al. [6]. The original model was fitted using pure silver. To meet the specifications of an industrial setting, the model was reparameterised using a promoted silver dispersed in α-alumina catalyst.

E^{forw} and $k^{forw,T_{ref}}$ for all the rate-limiting step (2, 5, 7, 8, and 13) were estimated. The $\alpha_{ref}^{\rho_*}$ for catalyst loadings 2, 3, 4, and 6 were also estimated (Table 2). The quality of this result is specially visible for the EO dry outlet; for example, for catalyst loading 2, the standard deviation was 0.1 %.

Equally important was to introduce other effects to the model which are ubiquitous in the industry. For this purpose, the last phase of this work investigated feasible extensions to the current model. Firstly, the moderator effect was considered of the utmost relevance. A discussion on conceivable approaches to incorporate this phenomenon was completed. Competitive adsorption and Ag-bonding were selected as the most feasible options.

Studying the implementation of catalyst deactivation in the model equally suited the objective of obtaining a comprehensive industrial reactor model, since deactivation is a source of concern in this process. Deactivation is commonly balanced with coolant temperature elevation to maintain equal conversion in time. These efforts are a short-term solution, to extend catalyst lifetime before replacement becomes imperative.

A deactivation expression was developed for the current microkinetic model. A sensitivity analysis was performed to test the quality of the incorporated effect and viable kinetic parameters were suggested using generic data. The site density deactivation was found reasonable when using $k_{d,0}^{\rho_*}$ = 4 x 10^{11} months^{-1} and $E_d^{\rho_*}$ = 155 kJ/mol. These values were selected to reproduce the Zhou and Yuan's [33] observed 35°C coolant temperature increase in 48 months. These parameters correspond to a drop in conversion from 10 % to 4 % and negligible change in the EO selectivity at constant coolant temperature.

Values for the combustion deactivation's E_d^{comb} were tested to observe if different trends are achievable for the selectivity. EO selectivities of 91 %, 90 %, and 89 % were obtained (for 150, 155 and 160 kJ/mol, respectively) at the end of the 48-month time horizon. The contribution of the combustion deactivation on the conversion decrease was considered negligible compared to the site density's. The main conclusion was that these three combustion deactivation activation energies produce very different plots, thus demonstrating that the selectivity trends from future data are attainable.

Overall the goal of this work was completed. Microkinetics were simulated within a high-fidelity reactor model. Several conclusions were drawn from the various simulations. Moreover, the model was enhanced to meet the specifications of the industrial production of ethylene oxide.

Future Work

This work adapted Stegelmann et al.'s model [6] to be applicable to an industrial catalyst and conditions. This adaptation was established through parameter estimations using experimental data. Validation of these estimated parameters with other experimental trials would prove the quality of the enhanced model.

Adding trials which co-feed EO in the absence of ethylene to the parameter estimation would also help verify the extent of the ethylene oxide combustion, and its corresponding contribution to the carbon dioxide and water production. This would further validate the estimated parameters.

Additionally, to obtain a clear idea of the ethylene combustion route, supplementary experiments could be performed to trace intermediates. This would substantiate the outlined route or supply an alternative viable explanation. If an alternative route is outlined, the kinetic parameters should be determined using the original method elaborated by Stegelmann et al. [6], statistical thermodynamics using gas molecules and adsorbates.

In the *Model Extensions* section, the scheme was tested within a multitubular catalytic fixed bed reactor model. Given that the parameters have now been refined, it would be intriguing to test their quality against industrial data. With industrial data of the components and temperature profiles, a comparison could be made between the performance of the detailed kinetics against the conventional rate-expression models.

Regarding the moderator effect, future work could consist in testing the Ag-bonding theory for VCM moderation.

The starting point for determining the sets of parameters is suggested to be the values of the original model. Preferably, more data on surface science could be collected to prove/disprove this theory, along with possible intermediates and adsorption enthalpy values, before entering this stage.

Van Hoof et al. and other authors [53, 54] have recently discovered (through STEM analysis) the importance of the size and shape of the silver particles in the epoxidation reaction. Thus, it would be preferable to create a more complex formulation of the site density variable, to account for shape and size of silver particles.

Upon validating the proposed moderator effect, this model could be used to optimise the reactor's performance. This could include finding the optimal quantity of moderator to add to the reactor's feed which is dependent on the moderator coverage of the catalyst's surface [46, 47, 50].

The catalyst deactivation model extension would also benefit from a parameter estimation, since only feasible values were proposed in the *Model Extensions* section (to uncover if this phenomenon could be incorporated in the model).

A first approach could consist in applying the presented expressions to the experiments considered in the *Parameter Estimation* and conclude if the fit could be improved by inserting catalyst deactivation. The estimations should begin by using merely site density deactivation, and only add the combustion deactivation if the selectivity trends are seen to be notably modelled worse than the conversion. A second stage would be to extend this approach to other experiments.

From the quality of the fit, interesting illations could be drawn. Namely, weather the proposed deactivation expressions are qualified to model the catalyst's decay, or if other aspects have an acute impact in deactivation as well. Moreover, due to the uncertainty of how the moderator interferes with the surface reaction, the catalyst undergoing changes due to its presence, namely poisoning (a reversible deactivation contribution) is a valid possibility [49, 53, 55]. This would, once more, call for the more complex formulation of the site density variable.

Acknowledgments

Acknowledgment is made to Petkim Petrokimya Holding A.Ş. for providing the experimental trials that furthered the analysis of the ethylene epoxidation reaction scheme.

References

[1] L. Schmidt, M. Huff, S. S. Bharadwaj, *Chem. Eng. Sci.* **49**, 3981 (1994).

[2] A. Andreasen, H. Lynggaard, C. Stegelmann, P. Stoltze, *Appl. Catal. A-Gen.* **289**, 267 (2005).

[3] S. Rebsdat, D. Mayer, *Ullmann's Encyclopedia of Industrial Chemistry* (Wiley, 2011), 7th edn.

[4] S. Aryana, M. Ahmadi, V. Gomes, J. Romagnoli, K. Ngian, *Chem. Prod. Process Model.* **4** (2009).

[5] O. Deutschmann, H. Knözinger, K. Kochloefl, T. Turek, *Ullmann's Encyclopedia of Industrial Chemistry* (Wiley, 2011), 7th edn.

[6] C. Stegelmann, N. C. Schiødt, C. T. Campbell, P. Stoltze, *J. Catal.* **221**, 630 (2004).

[7] D. Lafarga, M. A. Al-Juaied, C. M. Bondy, A. Varma, *Ind. Eng. Chem. Res.* **39**, 2148 (2000).

[8] Z. Nawaz, *Chem. Eng. Technol.* **39** (2016).

[9] L. Petrov, A. Eliyas, D. Shopov, *Appl. Catal.* **24**, 145 (1986).

[10] J. T. Salmi, M. Roche, J. H. Carucci, K. Eränen, D. Murzin, *Curr. Opin. Chem. Eng.* **1**, 321–327 (2012).

[11] V. Russo, T. Kilpiö, J. H. Carucci, M. Di Serio, J. T. Salmi, *Chem. Eng. Sci.* **134**, 563 (2015).

[12] E. P. S. Schouten, P. Borman, K. R. Westerterp, *Chem. Eng. Process.* **35**, 43 (1996).

[13] E. P. S. Schouten, P. Borman, K. R. Westerterp, *Chem. Eng. Process.* **35**, 107 (1996).

[14] P. Borman, K. R. Westerterp, *Ind. Eng. Chem. Res.* **34**, 49 (1995).

[15] Y. Jun, D. Jingfa, Y. Xiaohong, Z. Shi, *Appl. Catal. A-Gen.* **92**, 73 (1992).

[16] C. Chen, J. Harris, A. Bhan, *Chem. Eur. J.* **24**, 12405 (2018).

[17] R. B. Grant, R. Lambert, *J. Catal.* **92**, 364 (1985).

[18] V. I. Bukhtiyarov, *et al.*, *J. Catal.* **238**, 260 (2006).

[19] R. A. van Santen, H. P. C. E. Kuipers, *Adv. Catal.* **35**, 265 (1987).

[20] T. E. Jones, *et al.*, *ACS Catal.* **8**, 3844 (2018).

[21] N. Kenge, S. Pitale, K. Joshi, *Surf. Sci.* **679**, 188 (2019).

[22] K. C. Waugh, M. Hague, *Catal. Today* **157**, 44 (2010).

[23] M. Özbek, R. van Santen, *Catal. Lett.* **143**, 131–141 (2013).

[24] M. Özbek, I. Onal, R. van Santen, *ChemCatChem* **3**, 150 (2011).

[25] S. Linic, M. Barteau, *J. Catal.* **214**, 200 (2003).

[26] E. L. Force, A. T. Bell, *J. Catal.* **40**, 356 (1975).

[27] B. Partopour, A. Dixon, *AlChE J.* **63**, 87 (2017).

[28] A. Lukaski, M. Barteau, *Catal. Lett.* **128**, 9 (2009).

[29] H. H. Kung, *Chem. Eng. Commun.* **118**, 17 (1992).

[30] D. M. Minahan, G. B. Hoflund, W. S. Epling, D. W. Schoenfeld, *J. Catal.* **168**, 393 (1997).

[31] M. C. N. A. de Carvalho, F. Passos, M. Schmal, *J. Catal.* **248**, 124 (2007).

[32] T. C. Rocha, M. Hävecker, A. Knop-Gericke, R. Schlögl, *J. Catal.* **312**, 12 (2014).

[33] X. Zhou, W. Yuan, *Chem. Eng. Process.* **44**, 1098 (2005).

[34] N. Luo, W. Du, Z. Ye, F. Qian, *Ind. Eng. Chem. Res.* **51**, 6926–6932 (2012).

[35] A. Eliyas, L. Petrov, D. Shopov, *Appl. Catal.* **41**, 39 (1988).

[36] G. Boskovic, N. Dropka, D. Wolf, A. Brückner, M. Baerns, *J. Catal.* **226**, 334 (2004).

[37] C. Stegelmann, P. Stoltze, *J. Catal.* **226**, 129 (2004).

[38] D. Stacchiola, G. Wu, M. Kaltchev, W. Tysoe, *Surf. Sci.* **486**, 9 (2001).

[39] B. Krüger, G. Benndorf, *Surf. Sci.* **178**, 704 (1986).

[40] E. L. Force, A. T. Bell, *J. Catal.* **38**, 440 (1975).

[41] C. T. Campbell, M. T. Paffett, *Surf. Sci.* **139**, 396 (1984).

[42] C. T. Campbell, M. T. Paffett, *Appl. Surf. Sci.* **19**, 28 (1984).

[43] C. T. Campbell, B. E. Koel, *J. Catal.* **92**, 272 (1985).

[44] C. T. Campbell, *J. Catal.* **99**, 28 (1986).

[45] Ş. Sarrafi, Development of Kinetic Model for Industrial Ethylene Oxide Catalyst by Using Model-Targeted Experimentation Approach, Master of Science in Chemical Engineering, Graduate School of Engineering and Sciences of Izmir Institute of Technology (2019).

[46] J. Harris, A. Bhan, *J. Catal.* **367**, 62 (2018).

[47] D. Kamenski, N. V. Kulkova, D. Bonchev, *Reaction Kinetics and Catalysis Letters* **7**, 481 (1977).

[48] H. E. Al-Ahmadi, A. S. Padia, Epoxidation on process with added moderator (2015).

[49] M. Argyle, C. Bartholomew, *Catalysts* **5**, 145 (2015).

[50] G. Boskovic, D. Wolf, A. Brückner, M. Baerns, *J. Catal.* **224**, 187 (2004).

[51] X. Zhou, W. Yuan, *Chem. Eng. Sci.* **59**, 1723 (2004).

[52] C. H. Bartholomew, *Appl. Catal. A-Gen.* **212**, 17 (2001).

[53] A. J. F. van Hoof, I. Filot, H. Friedrich, E. J. M. Hensen, *ACS Catal.* **8**, 11794–11800 (2018).

[54] P. Christopher, S. Linic, *ChemCatChem* **2**, 78 (2010).

[55] K. Kumbilieva, L. Petrov, Y. Alhamed, A. Alzahrani, *Chin. J. Catal.* **32**, 387–404 (2011).